BJP British Journal of Pharmacology

DOI:10.1111/j.1476-5381.2011.01458.x
www.brjpharmacol.org

RESEARCH PAPER

Cyclopeptide RA-V inhibits angiogenesis by down-regulating ERK1/2 phosphorylation in HUVEC and HMEC-1 endothelial cells

Grace GL Yue[1,4], Jun-Ting Fan[3], Julia KM Lee[1,4], Guang-Zhi Zeng[3], Tina WF Ho[1,4], Kwok-Pui Fung[1,2,4], Ping-Chung Leung[1,4], Ning-Hua Tan[3] and Clara BS Lau[1,4]

[1]*Institute of Chinese Medicine and* [2]*School of Biomedical Sciences, The Chinese University of Hong Kong, Shatin, New Territories, Hong Kong, China,* [3]*State Key Laboratory of Phytochemistry and Plant Resources in West China, Kunming Institute of Botany, Chinese Academy of Sciences, Kunming, China, and* [4]*State Key Laboratory of Phytochemistry and Plant Resources in West China, The Chinese University of Hong Kong, Shatin, New Territories, Hong Kong, China*

Correspondence
Clara BS Lau, Institute of Chinese Medicine, The Chinese University of Hong Kong, Shain, New Territories, Hong Kong, China. E-mail: claralau@cuhk.edu.hk; Ning-Hua Tan, State Key Laboratory of Phytochemistry and Plant Resources in West China, Kunming Institute of Botany, Chinese Academy of Sciences, Kunming, China. E-mail: nhtan@mail.kib.ac.cn

Keywords
cyclopeptide; RA-V; angiogenesis; ERK1/2; *Rubia yunnanensis*; HUVEC; HMEC-1; endothelial cells

Received
12 December 2010
Revised
6 April 2011
Accepted
18 April 2011

BACKGROUND AND PURPOSE
Anti-angiogenic agents have recently become one of the major adjuvants for cancer therapy. A cyclopeptide, RA-V, has been shown to have anti-tumour activities. Its *in vitro* anti-angiogenic activities were evaluated in the present study, and the underlying mechanisms were also assessed.

EXPERIMENTAL APPROACH
Two endothelial cell lines, human umbilical vein endothelial cells (HUVEC) and human microvascular endothelial cells (HMEC-1), were used. The effects of RA-V on the proliferation, cell cycle phase distribution, migration, tube formation and adhesion were assessed. Western blots and real-time PCR were employed to examine the protein and mRNA expression of relevant molecules.

KEY RESULTS
RA-V inhibited HUVEC and HMEC-1 proliferation dose-dependently with IC_{50} values of 1.42 and 4.0 nM respectively. RA-V inhibited migration and tube formation of endothelial cells as well as adhesion to extracellular matrix proteins. RA-V treatment down-regulated the protein and mRNA expression of matrix metalloproteinase-2. Regarding intracellular signal transduction, RA-V interfered with the activation of ERK1/2 in both cell lines. Furthermore, RA-V significantly decreased the phosphorylation of JNK in HUVEC whereas, in HMEC-1, p38 MAPK was decreased.

CONCLUSIONS AND IMPLICATIONS
RA-V exhibited anti-angiogenic activities in HUVEC and HMEC-1 cell lines with changes in function of these endothelial cells. The underlying mechanisms of action involved the ERK1/2 signalling pathway. However, RA-V may regulate different signalling pathways in different endothelial cells. These findings suggest that RA-V has the potential to be further developed as an anti-angiogenic agent.

Abbreviations
Ang, angiopoietin; ECM, extracellular matrix; FBS, fetal bovine serum; GAPDH, glyceraldehyde-3-phosphate dehydrogenase; HMEC-1, human microvascular endothelial cells; HUVEC, human umbilical vein endothelial cells; MTT, 3-(4,5-dimethylthiazol-2-yl)-2,5-diphenyl-tetrazolium bromide; PI3K, phosphatidylinositol 3-kinase

Introduction

Cancer is an angiogenesis-dependent disease (Folkman, 1971, 2007) and blocking such angiogenesis is an accepted strategy to arrest tumour growth and metastasis (Carmeliet and Jain, 2000). Studies with the first angiogenesis inhibitors were reported in the 1980s (Taylor and Folkman, 1982; Crum *et al.*, 1985) And in the past two decades, additional angiogenesis inhibitors have been discovered and have completed clinical trials. For example, bevacizumab (a humanized antibody against VEGF-A) and bortezomib (a proteasome inhibitor with potent anti-angiogenic activity) have been approved for clinical use and are in different phases of clinical trials for other indications (Folkman, 2007). Anti-angiogenic therapies, which are aimed at suppressing new blood vessel growth, have the potential to become a new target focus or a major adjuvant for cancer treatment. Natural products, including traditional Chinese herbs, are rich source of angiogenesis-modulating compounds (Fan *et al.*, 2006). Some angiogenesis inhibitors have been isolated from natural products, such as Taxol® (*Taxus brevifolia*; Avramis *et al.*, 2001), camptothecin (*Camptotheca acuminate*; Clements *et al.*, 1999), combretastatin (*Combretum caffrum*; Vincent *et al.*, 2005), triptolide (*Tripterygium wilfordii*; He *et al.*, 2010) and farnesiferol C (*Ferula assafoetida*; Lee *et al.*, 2010a).

RA-V (deoxybouvardin) is a cyclopeptide isolated from *Rubia yunnanensis* (family Rubiaceae). The plant is widely distributed and used as anti-tumour herb in folk remedies in Yunnan province of China. Rubiaceae-type cyclopeptides (RAs) were isolated from *Bouvardia ternifolia* (Cav.) Schlecht. and *Rubia cordifolia* L. in the '70s and '80s (Jolad *et al.*, 1977; Itokawa *et al.*, 1983, 1984a,b; Tan and Zhou, 2006). Several RAs have been shown to have potent anti-tumour activities in mouse cancer cells and tumours, such as P-388 and L1210 leukaemia and ascite tumours, B-16 melanoma, colon 38 adenocarcinoma, Lewis lung carcinoma and Ehrlich carcinoma (Itokawa *et al.*, 1983, 1984a, 1993). The strong anti-tumour activity of RA-V was demonstrated in mouse MM2 mammary carcinoma *in vivo*. Treatment with RA-V (0.05–10 mg kg^{-1}) also prolonged the life span of mice with P-388 or L1210 leukaemia (Itokawa *et al.*, 1984a). Recent studies on RA-V demonstrated the inhibition of NO production and anti-tumour activities in mouse peritoneal macrophages (Tao *et al.*, 2003) and mouse P-388 leukaemia cells (Lee *et al.*, 2008) respectively. Furthermore, RA-V could significantly inhibited TNF-α-induced NF-κB activation in HEK-293-NF-kB luciferase stable cells with IC_{50} values of 0.03 μM (Fan *et al.*, 2010). On the other hand, RA-V has been shown to inhibit proliferation of bovine aortic endothelial cells and HUVEC (Koizumi *et al.*, 2006). Nevertheless, the underlying mechanisms of the anti-angiogenic effects of RA-V remain unknown.

The present study aimed to investigate the anti-angiogenic effects of RA-V in two human endothelial cell lines and elucidate its mechanisms of action. Many studies have demonstrated the heterogeneity of endothelial cells (Conway and Carmeliet, 2004; Aird, 2007), so that experiments performed on one type of endothelial cells may be misleading (Nanobashvili *et al.*, 2003). Therefore, human umbilical vein endothelial cells (HUVEC) and human dermal microvascular endothelial cells (HMEC-1) were used in this study to evaluate the cellular responses towards RA-V. The former are macrovascular cells, while the latter are microvascular cells, and their angiogenic potency and sensitivity to growth factors were shown to be different (Nanobashvili *et al.*, 2003; Aird, 2007). Our results demonstrated that RA-V possessed anti-angiogenic effects in both HUVEC and HMEC-1 cells, and the ERK1/2 signalling pathway was involved in these activities of RA-V.

Methods

Extraction and isolation procedures for RA-V

The air-dried and powdered roots of *R. yunnanensis* (100 kg) were extracted three times with methanol (3 × 100 L). After removal of the solvent under vacuum, the methanol extract (21 kg) was suspended in water and partitioned successively with ethyl acetate and *n*-butanol respectively. The ethyl acetate fraction (6.4 kg) was subjected to silica gel column chromatography eluted with $CHCl_3$–methanol (1:0, 95:5, 9:1, 8:2, 0:1) to afford five fractions. Fractions that contained cyclopeptides (1.2 kg, $CHCl_3$–methanol, 95:5, 9:1, 8:2) were combined and again re-chromatographed on a silica gel column eluting with a $CHCl_3$–methanol gradient system (70:1–8:2) to yield six fractions (Fr. 1 to Fr. 6). Fr. 1 (139 g) was analysed on silica gel columns, eluting with petroleum ether–acetone (7:3–0:1) to furnish five subfractions (Fr. 1–1 to Fr. 1–5). Fr. 1–4 (30 g) was chromatographed on Sephadex LH-20 ($CHCl_3$–methanol, 1:1) and then purified by repeated passage through silica gel H, eluting with petroleum ether–acetone (6:4) to afford RA-V (4 g, 0.004% w/w). The identification of the purified compound was based on the ^1H and ^{13}C NMR spectral analysis and mass spectrometry.

Cell culture

The HUVEC were maintained in DMEM/F12 medium containing 10% v/v heat-inactivated FBS, 100 units mL^{-1} penicillin–streptomycin, 100 μg mL^{-1} heparin and 30 μg mL^{-1} endothelial cell growth supplement. The HMEC-1 were maintained in MCDB 131 medium containing 10% v/v FBS, 100 units mL^{-1} penicillin–streptomycin, 2 mM glutamine, 1 μg mL^{-1} hydrocortisone and 10 ng mL^{-1} EGF. The pancreatic cancer cells (Panc-1 and SW1990) were maintained in Dulbecco's modified Eagle's medium (DMEM), while Capan-1 cells were maintained in Iscove's modified Dulbecco's medium (IMDM). The cancer cell media were supplemented with 10% v/v FBS and 100 units mL^{-1} penicillin–streptomycin. The cells were incubated at 37°C in a humidified atmosphere of 5% CO_2. When the cells reached 80% confluence in the culture flask, trypsin–EDTA was used to remove the cells, and the cells were used in experiments or reseeded in flask. RA-V was prepared at 100 mM in dimethyl sulphoxide (DMSO) and stored at –20°C and reconstituted in appropriate media before the experiments.

Cell proliferation and cytotoxicity assay

The endothelial cells (HUVEC, HMEC-1, 3×10^4 cells mL^{-1}) or cancer cells (Panc-1, SW1990, Capan-1, 5×10^4 cells mL^{-1}) were seeded in 96-well flat-bottom culture plates (Iwaki, Japan) with 100 μL culture medium and incubated overnight.

Subsequently, 100 µL culture media containing various concentrations (1.25–20 nM for endothelial cells; 1.25–200 nM for cancer cells) of RA-V were added into the wells. Then the plates were incubated at 37°C for 48 h. Plain medium containing vehicle solvent (0.5% v/v DMSO) were added to the control wells.

The effects of RA-V on the proliferation of HUVEC and HMEC-1 were determined by [methyl-^{3}H]-thymidine incorporation. The cytotoxicities of RA-V on the endothelial cells and cancer cells were assessed by MTT assay. The procedures of thymidine incorporation and MTT assay have been described in detail in an earlier study (Yue *et al.*, 2010).

Cell cycle analysis

The HUVEC or HMEC-1 (1×10^5 cells mL^{-1}) were seeded at 6-well culture plates and incubated overnight. The cells were treated with RA-V at 10 or 20 nM for 48 or 72 h in four different conditioned media: basal medium (with FBS but no growth factors), basal medium with VEGF (10 ng mL^{-1}), basal medium with basic fibroblast growth factor (bFGF; 50 ng mL^{-1}) and medium without FBS and growth factors. Cells were harvested after incubation and subjected to propidium iodide (PI) flow cytometry analysis as described by Yue *et al.*, (2010).

Tube formation assay

Formation of capillary tube like structures by HUVEC and HMEC-1 was assessed in Matrigel-based assay. Briefly, a 96-well plate coated with 60 µL of Matrigel per well was allowed to solidify at 37°C for 1 h. Cells (1.5×10^4 in 100 µL medium) were added to each well, and 100 µL of medium containing 10 or 20 nM of RA-V was added and incubated for different periods of time. The tube formation of endothelial cells was examined in four different conditioned-media as described in previous section. Each treatment was performed in triplicate. The enclosed networks of tubes were photographed under a microscope (Olympus IX-71, Center Valley, PA, USA). The total tube lengths of the tube structure of each photograph were measured using Image-Pro Plus 6.0 software (Media Cybernetics, Bethesda, MD, USA). Inhibition of tube formation was calculated as tube length (treated) over tube length (control) (Zhang *et al.*, 2006; Kimura *et al.*, 2008).

Cell migration assay

To assess the cell migration ability of HUVEC and HMEC-1, a modified Boyden chamber assay was used. Cells (3×10^4 in 100 µL medium) were added into each transwell filter chamber with 8 µm pore size (Corning, Lowell, MA, USA). At the same time, 100 µL of medium containing various concentrations of RA-V (with 1% v/v FBS) was added to the upper chambers. Five hundred microlitres of medium (with 10% v/v FBS), served as chemoattractant media, was added to the lower chambers. The cells were allowed to migrate through the 8 µm pore to the lower chamber for 5–6 h at 37°C, 5% CO_2. After incubation, cells were fixed with methanol and stained with haematoxylin. Cells on the top surface of the filter membrane (non-migrated) were scraped with cotton swab. Stained filters were photographed under microscope (Olympus IX-71). The migrated cells were quantified by manual counting (Xiao and Singh, 2007). Changes in cell numbers are represented as a percentage of control values.

The cell motility of HUVEC and HMEC-1 was also evaluated using a scratch wound assay. Cells (1×10^5 in 1 mL medium) were added into each well of 24-well plate and cultured overnight. The cells were starved with 1% v/v FBS medium for 24 h. The cells were then scraped with a cross in the middle of well with 200 µL pipette tips. After scraping the cells, the medium was changed with fresh medium with 10 or 20 nM of RA-V. The cells were incubated for different time intervals (16 or 24 h), and each well was photographed under a microscope (Olympus IX-71). The percentages of open wound area were measured and calculated using the TScratch software (Vigl *et al.*, 2009). Motility was determined by the decrease in open wound area.

Extracellular matrix cell (ECM) adhesion assay

Cell adhesion of HUVEC and HMEC-1 was assessed using the Extracellular Matrix Cell Adhesion Array Kit (Chemicon, Millipore, Billerica, MA, USA). Each eight-well strip consists of wells pre-coated with seven different human ECM proteins (collagen I, collagen II, collagen IV, fibronectin, laminin, tenascin and vitronectin) and one BSA-coated well (negative control). The assay was carried out according to the procedures recommended in the assay kit manual. The change in optical density was represented as fold of control (without RA-V).

Western blot analysis

Human endothelial cells HUVEC and HMEC-1 (1×10^6 cells mL^{-1}) were seeded in 100 mm culture dish and incubated for 24 h to allow attachment. Various concentrations (10 or 20 nM) of RA-V were added to the dishes and incubated for 24 or 48 h. For the measurement of NF-κB activation, endothelial cells were pre-incubated with 10 or 20 nM of RA-V for 3 h and treated with 10 ng mL^{-1} TNF-α for 30 min. After treatment, attached and floating cells were harvested and washed twice with PBS. The cell pellets were then lysed with whole cell extraction buffer (2% SDS, 10% glycerol, 625 mM Tris–HCl, pH 6.8) for 15 min on ice. The samples were heated at 95°C for 10 min and then centrifuged at 14 000× *g* for 20 min at 4°C. The supernatant proteins were resolved by 12% SDS-polyacrylamide gel and transferred to 0.45 µm PVDF membrane (Immobilon, Millipore). The membrane was blocked with 5% non-fat milk in Tris-buffered saline containing Tween-20 (20 mM Tris–HCl, pH 7.6, 150 mM NaCl, 0.1% Tween-20). The blots were incubated overnight with primary antibodies against human β-actin (Sigma, St. Louis, MO, USA), MMP2, MMP9, VEGFR1, phospho-VEGFR2 (pVEGFR2), Tie2, ERK1/2, pERK, JNK, pJNK, p38, pp38, PI3, pPI3, NFκB, IκB, pIκB (Cell Signalling, Danvers, MA, USA), p21, cyclin B1 and cyclin D1 (BD Biosciences, San Diego, CA, USA). After incubation with the secondary horseradish peroxidase-conjugated antibodies (Invitrogen, Carlsbad, CA, USA) for 1 h, detection was performed using enhanced chemiluminescence assay kit (GE Healthcare, UK).

Real-time PCR analysis

Human endothelial cells HUVEC and HMEC-1 (1×10^6 cells mL^{-1}) were seeded in 100 mm culture dishes and incubated

for 24 h to allow attachment. Various concentrations (10 or 20 nM) of RA-V were added to the dishes and incubated for 24 or 48 h. After treatment, cells were harvested, washed twice with cold PBS and collected by scraping. Total RNA was extracted from cells using Trizol reagent according to the manufacturer's protocols. The RNA concentration was spectrophotometrically determined using a BioPhotometer (Eppendorf, Germany). Reverse transcription of the 3 μg total RNA was performed in Bio-Rad iCycler (Bio-Rad, Hong Kong) using SuperScript III Reverse Transcriptase reagents according to the manufacturer's protocols. To quantify the amount of mRNA of *Ang 1*, *Ang 2*, *Tie 2*, *VEGFR2*, *MMP2* and *MMP9*, real-time semi-quantitative PCR of cDNA samples were performed in Bio-Rad CFX96™ Real-time system C1000 Thermal cycler using the iTaq Fast SYBR Green Supermix from Bio-Rad. Each 20 μL PCR sample contained 80 ng cDNA, 10 μL Supermix, RNase-free water and 1.25 μL of both the specific forward and reverse primers (10 mM), which were synthesized by Invitrogen. The sequences of the primers are listed in the supplementary file Table S1. Reactions were performed in triplicate using the following protocol: 3 min pre-incubation at 95°C, followed by 40 PCR cycles at 95°C for 3 s, 60°C for 30 s, and 72°C for 5 s. Relative quantification was obtained by the comparative threshold cycle (ΔΔCt) method (CFX Manager Software, version 1.6, Bio-Rad). The specific gene mRNA levels were normalized relative to GAPDH mRNA level in each sample.

In vivo *Matrigel plug assay*

All animal care and experimental procedures complied with the guidelines of the Animal Experimentation Ethics Committee of the Chinese University of Hong Kong. Male C57BL/6 mice (6 weeks old) were supplied and maintained by Laboratory Animal Service Center, the Chinese University of Hong Kong. Matrigel (500 μL) was mixed with heparin (10 U/mL), VEGF 100 ng/mL and RA-V (100 or 500nM) prior to s.c. injections into the flanks of mice. Negative controls were obtained by injecting mice with Matrigel without VEGF and RA-V. After 7 days, the Matrigel plugs were removed and photographed. The haemoglobin content of the Matrigel plugs was quantified using Drabkin's reagent kit (Sigma). Haemoglobin content was expressed as mg mg^{-1} of wet Matrigel plug (Chia *et al.*, 2010; Lee *et al.*, 2010b).

Statistical analysis

Data are expressed as mean + SD. Statistical analyses and significance, as measured by the Student's *t*-test for paired samples, were performed using GraphPad PRISM software version 5.0 (GraphPad Software, La Jolla, CA, USA). In all comparisons, $P < 0.05$ was considered statistically significant.

Materials

The roots of *R. yunnanensis* were commercially purchased from the Yunnan Lv-Sheng Pharmaceutical Co. Ltd, Kunming, China. The material was identified by Prof Su-Gong Wu at Kunming Institute of Botany. A voucher specimen (no. Wu20070905) has been deposited in the Herbarium of Kunming Institute of Botany, Chinese Academy of Sciences, China.

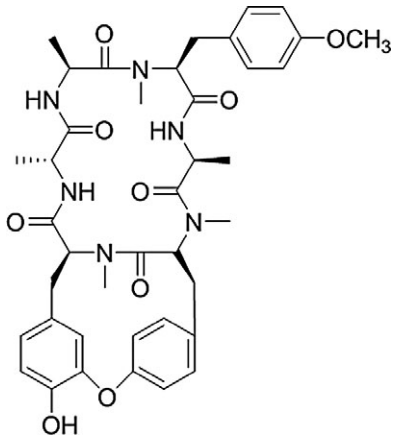

Figure 1
Chemical structure of RA-V.

HUVEC, HMEC-1 and human pancreatic cancer cells (Panc-1, SW1990, Capan-1) were purchased from American Type Culture Collection (Manassas, VA, USA). DMEM/F12, DMEM, IMDM, fetal bovine serum (FBS), penicillin–streptomycin, trypsin–EDTA, recombinant VEGF, Trizol, SuperScript III Reverse Transcriptase, dNTP were obtained from Invitrogen. MCDB 131 medium, endothelial cell growth supplement, EGF, bFGF, hydrocortisone, heparin, gelatin, haematoxylin, MTT and Drabkin's reagent were obtained from Sigma. Basement membrane matrix Matrigel (growth factor reduced) was from BD Biosciences. [Methyl-^{3}H]-thymidine and Unifilters were from PerkinElmer (Waltham, MA, USA). Real-time PCR reagent iTaq Fast SYBR Green Supermix was from Bio-Rad. Transwell polycarbonate cell culture inserts (6.5 mm diameter, 8 μm pore size) were from Corning (Lowell, MA, USA). Receptor nomenclature follows Alexander *et al.* (2009).

Results

Structure elucidation of RA-V

The structure of RA-V was elucidated by ^{1}H and ^{13}C NMR spectroscopic analysis and positive FABMS, and its purity was found to be >99% [Agilent 1100 HPLC, Zorbax Eslipse-C18, 4.6 × 150 mm, 5 μm, USA, MeOH–H_2O (80:20)]. Its molecular formula was established as $C_{40}H_{48}N_6O_9$ by its positive FABMS (*m/z* 757, $[M + H]^+$), and its ^{1}H and ^{13}C NMR spectral data were listed in the supplementary file Table S2, which were in accordance with the reported data in the literature (Bates *et al.*, 1983). The chemical structure of RA-V was shown in Figure 1.

Cytotoxicities of RA-V in cancer cells and endothelial cells

The cytotoxicities of RA-V in three pancreatic cancer cell lines (Panc-1, SW1990 and Capan-1) and two endothelial cell lines (HUVEC and HMEC-1) were assessed by MTT assay after 48 h incubation. The concentrations of RA-V producing 50% cell death on the cells were listed in Table 1. The cytotoxicities of

Table 1

Concentrations producing 50% growth inhibition (IC_{50}) of RA-V on cancer and endothelial cells

Cell lines	Cell types	IC_{50} (nM)
Capan-1	Human pancreatic carcinoma	67.4
Panc-1	Human pancreatic carcinoma	70.4
SW1990	Human pancreatic carcinoma	68.5
HUVEC	Human endothelial cells	65.0
HMEC-1	Human endothelial cells	7.8

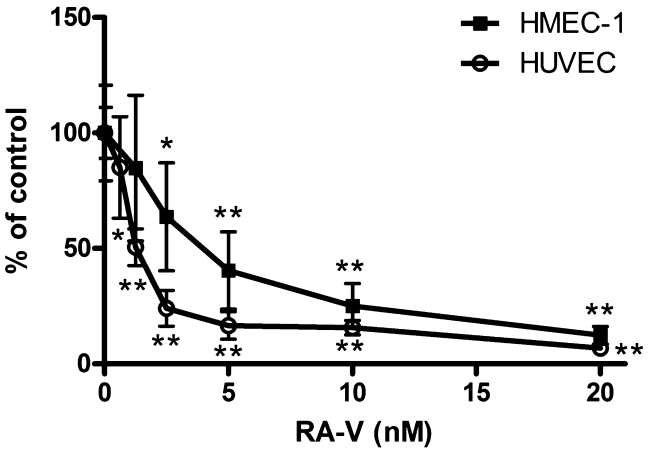

Figure 2

Effects of RA-V on proliferation of HUVEC and HMEC-1. Cells were treated with increasing concentrations of RA-V for 48 h, and cell proliferation viability was determined by the [^{3}H]thymidine incorporation assay. Results are expressed as the mean % ratio of count per minute in treated and untreated control cells (mean + SD of four independent experiments with five wells each). Differences between the treated and untreated control groups were determined by Student's unpaired *t*-test. *$P < 0.05$, **$P < 0.005$ significantly different from the control group.

RA-V in another 11 cancer cell lines have been evaluated by sulphorhodamine B assay in a previous study (Fan *et al.*, 2010). RA-V was shown to have the lowest IC_{50} values (~1 nM) in U251 (human glioma) and B16 (murine melanoma) cells. Such concentrations induce significant inhibition of growth, but not cytotoxicity, in endothelial cells.

Effects of RA-V on cell proliferation of endothelial cells

Different concentrations of RA-V were tested in HUVEC and HMEC-1 to examine its effect on the cell proliferation using the thymidine incorporation assay. As shown in Figure 2, RA-V (1.25–20 nM) was found to significantly inhibit the proliferation of HUVEC and HMEC-1 in a concentration-dependent manner after 48 h treatment. The concentrations producing 50% growth inhibition (IC_{50}) of RA-V on HUVEC and HMEC-1 were 1.42 and 4.00 nM respectively.

RA-V induced cell cycle arrest in endothelial cells

Cell cycle phases were detected by PI staining. HUVEC and HMEC-1 were exposed to 10 or 20 nM RA-V for 48 h or 72 h in four different conditioned media: basal medium, basal medium with VEGF (10 ng mL^{-1}), basal medium with bFGF (50 ng mL^{-1}) and medium without FBS and growth factors and analysed by flow cytometry. The data shown in Figure 3A and B represent four to six separate experiments. A concentration-dependent block in the G2/M phase of the cell cycle was observed in both cell lines. The RA-V-treated HUVEC in medium containing VEGF and bFGF were significantly arrested at G2/M phase after 48 and 72 h treatment ($P < 0.05$), while the population of G1 phase was significantly decreased after 72 h treatment (Figure 3C, D). In the absence of FBS and growth factors, RA-V (20 nM) treatment induced G2/M phase arrest of HUVEC at 48 h only but not at 72 h (Figure 3E). For the HMEC-1 in basal medium, medium containing bFGF and medium without FBS and growth factors, RA-V treatment significantly arrested G2/M phase and decreased G1 phase after 48 h and 72 h (Figure 3F–H).

RA-V inhibited tube formation in endothelial cells

Endothelial cells when seeded on three-dimensional matrix, such as Matrigel, are able to form capillary-like structure (Kimura *et al.*, 2008; Medhora *et al.*, 2008). Figure S1 shows the capillary-like tube formation following 16 h or 5 h treatments of HUVEC or HMEC-1 with DMSO (control, 0 nM) or different concentrations of RA-V respectively. The tube structures were visible in the control culture well coated with growth factor-reduced Matrigel. Treatment with RA-V disrupted tube formation of endothelial cells in different conditioned media. RA-V significantly inhibited the VEGF- and bFGF-induced capillary-like tube formation of HUVEC and HMEC-1 (Figure 4A, B, $P < 0.05$), while RA-V significantly inhibited the serum-induced tube formation in HMEC-1 only (Figure 4B). In the absence of FBS and growth factor, tube formation of HUVEC and HMEC-1 was inhibited by a higher concentration of RA-V (20 nM).

RA-V inhibited cell migration in endothelial cells

The effects of RA-V treatment on cell migration by endothelial cells were evaluated using a modified Boyden chamber assay (Figure 5A). In DMSO-treated control (0 nM), many endothelial cells migrated from the upper to lower chamber through the membrane after 6 h incubation, when the lower chamber contained culture medium supplemented with 10% v/v FBS as a chemoattractant. As shown in Figure 5B and C, RA-V (10 and 20 nM) blocked the migration of HUVEC and HMEC-1 in a concentration-dependent manner.

The effects of RA-V treatment on cell motility were also evaluated using the scratch wound assay (Figures 6, S2). Treatment of HUVEC and HMEC-1 with RA-V (10 and 20 nM) decreased cell motility compared with untreated cells in a concentration-dependent manner. The open wound areas in RA-V treated wells were significantly greater than those of untreated wells ($P < 0.05$) (Figure 6A, B).

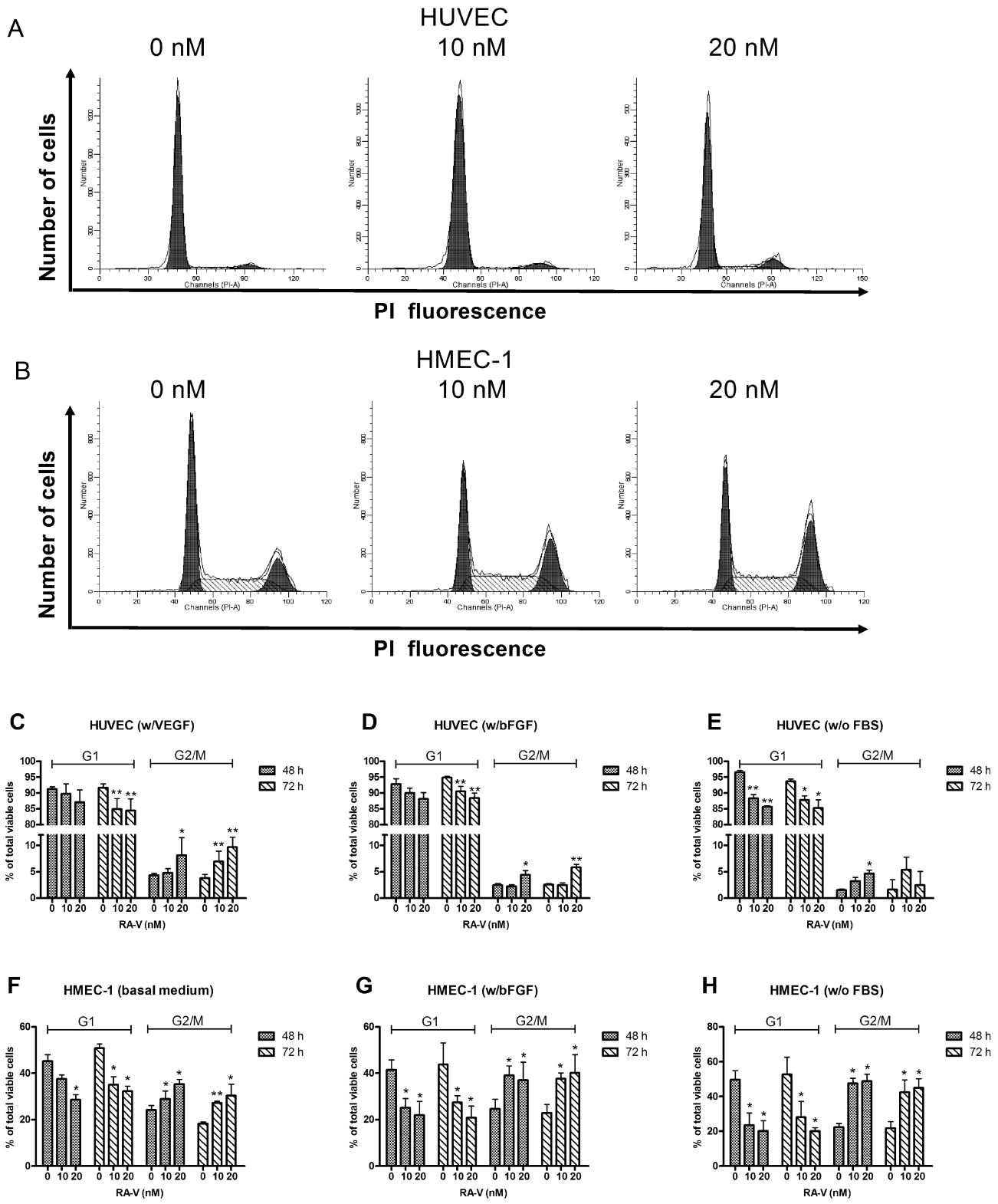

Figure 3

Effects of RA-V on cell cycle phase distribution of endothelial cells. Representative histograms showing the cell cycle analysis of HUVEC (A) and HMEC-1 (B) treated with vehicle or RA-V (10 or 20 nM) for 48 h. After treatment, cells were analysed by flow cytometry ($n = 4–6$). The fractions of cells in G1 and G2/M phase were summarized in bar charts (C–H). Results are expressed as the mean percentage of total viable cells in treated and untreated control cells (mean + SD). Differences between the treated and untreated control groups were determined by Student's unpaired *t*-test. *$P < 0.05$, **$P < 0.01$ significantly different from the control group.

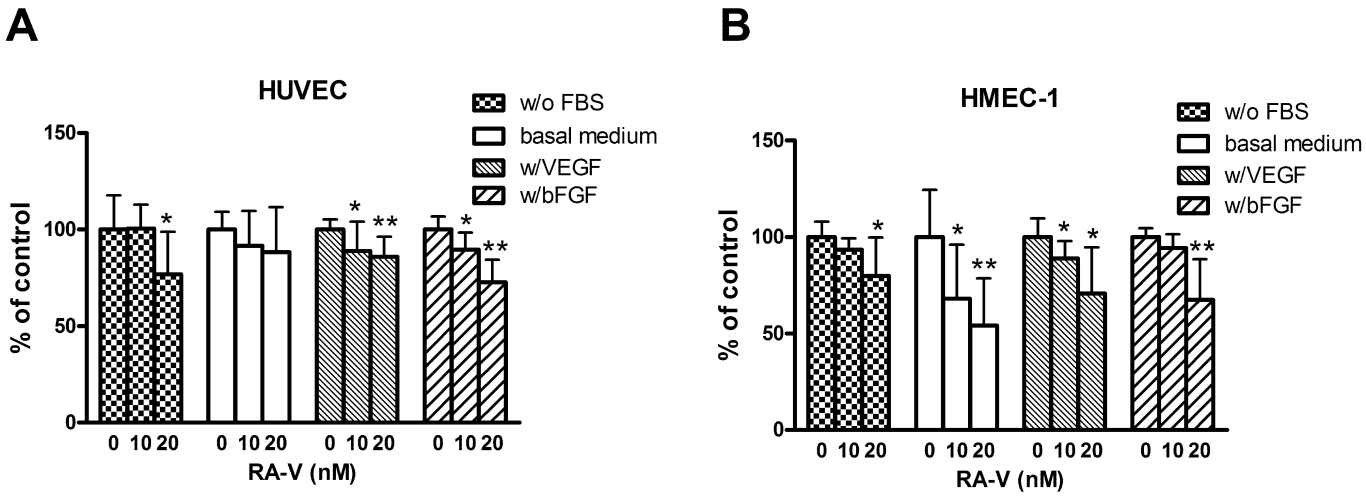

Figure 4

Effects of RA-V on capillary-like tube formation by HUVEC and HMEC-1. Quantification of tube formation in the presence or absence of FBS (10% v/v), or VEGF (10 ng mL^{-1}) or bFGF (50 ng mL^{-1}) in HUVEC (A) and HMEC-1 (B) were shown. Results are expressed as the mean percentage of control (mean + SD of three independent experiments with three wells each). Differences between the treated and untreated control groups were determined by Student's unpaired *t*-test. $^{*}P < 0.05$, $^{**}P < 0.01$ significantly different from the control group.

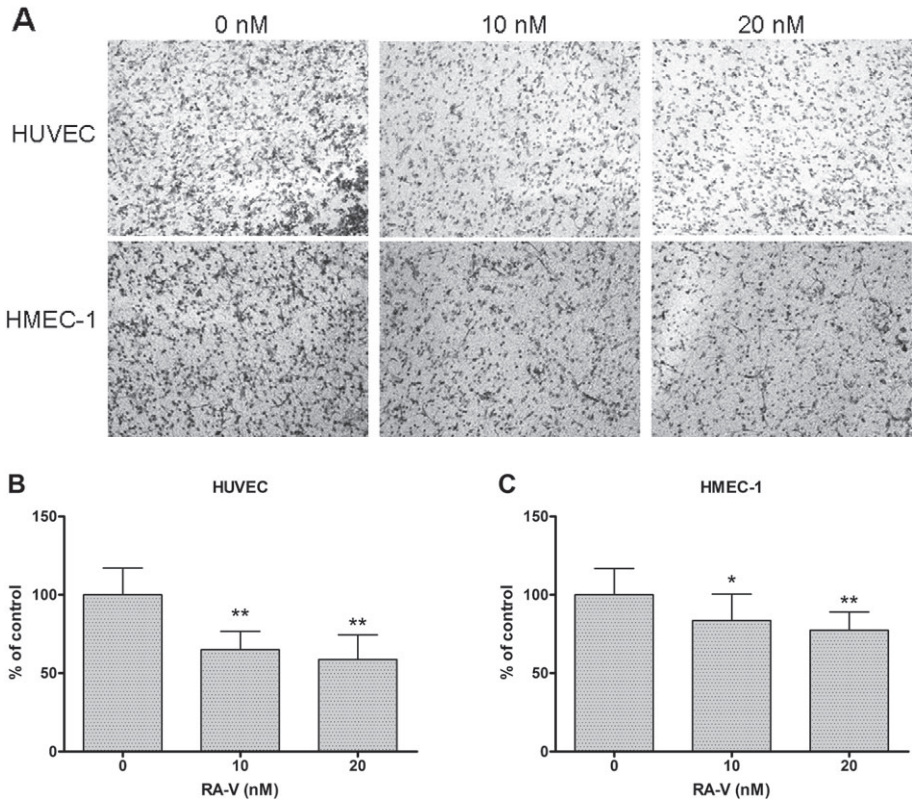

Figure 5

Effects of RA-V on migration of HUVEC and HMEC-1 in Boyden chambers. Representative photomicrographs showing the stained cells on the lower side of membranes (A). The cells in the upper chambers were treated with DMSO (control, 0 nM) or 10 or 20 nM RA-V. After 6 h incubation, those cells which had migrated to the lower chambers were stained and the numbers were counted. Quantification of cell migration in HUVEC (B) and HMEC-1 (C) were shown. Results are expressed as the mean percentage of control (mean + SD of three independent experiments with two wells each). Differences between the treated and untreated control groups were determined by Student's unpaired *t*-test. $^{*}P < 0.05$, $^{**}P < 0.01$ significantly different from the control group.

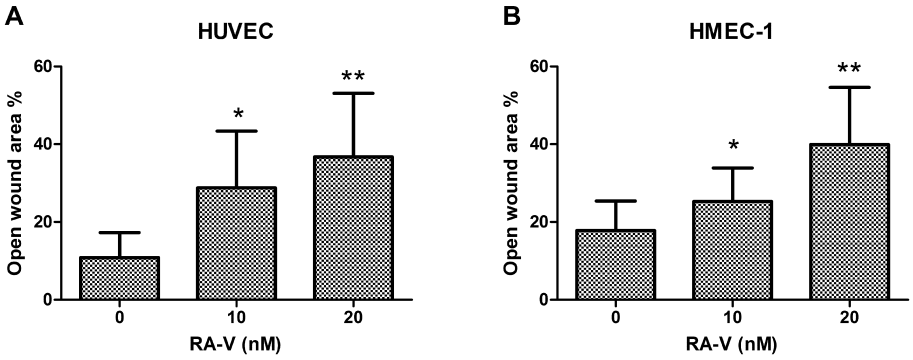

Figure 6

Effects of RA-V on wound-induced motility of HUVEC and HMEC-1. Quantification of cell motility in HUVEC (A) and HMEC-1 (B) were shown. Results are expressed in percentage of open wound remained after incubation (mean + SD of three independent experiments with three wells each). Differences between the treated and untreated control groups were determined by Student's unpaired *t*-test. $*P < 0.05$, $**P < 0.01$ significantly different from the control group.

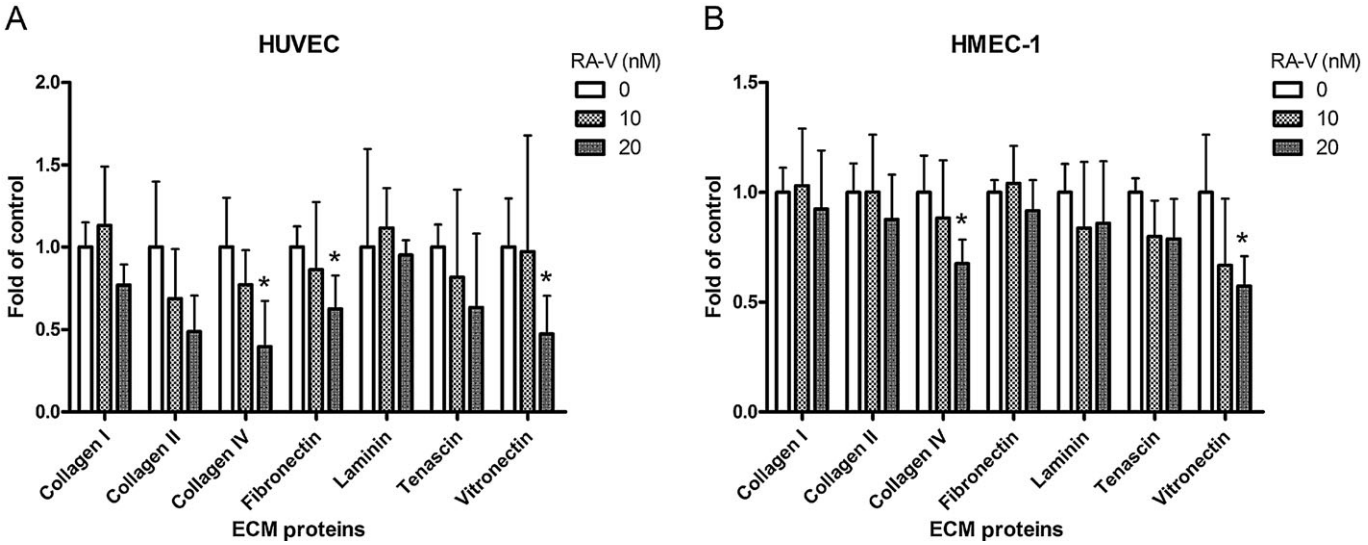

Figure 7

Effects of RA-V on cell adhesion of HUVEC (A) and HMEC-1 (B) to ECM proteins. Cells were added to a pre-coated plate containing different ECM proteins. The cells were allowed to adhere for 2 h at 37°C, and wells were washed to remove unbound cells. The attached cells were stained and the cell-bound stain was then extracted. The absorbance of the stain was determined. Results are expressed as the mean fold of untreated control wells (mean + SD of three independent experiments with duplicate well each). Differences between the treated and untreated control groups were determined by Student's unpaired *t*-test. $*P < 0.05$ significantly different from the control group.

RA-V decreased endothelial cells adhesion to matrix proteins

The cell adhesion of endothelial cells to different matrix proteins (collagen I, collagen II, collagen IV, fibronectin, laminin, tenascin and vitronectin) was assessed and the results showed that the cell adhesion to three matrix proteins decreased by RA-V treatment. The statistically significant decreases in adhesion were to collagen IV and vitronectin in both cell lines, while adhesion to fibronectin was only significantly decreased in HUVEC ($P < 0.05$, Figure 7A, B). Co-culture of HUVEC with RA-V (20 nM) resulted in 60%, 38% and 53% reduction of collagen IV, fibronectin and vitronectin adhesion respectively. Collagen I and II adhesions of HUVEC were decreased by 23% and 52%, respectively; however, the difference between RA-V treated and untreated control was not statistically significant ($P > 0.05$). The adhesion to collagen IV and vitronectin of HMEC-1 was also decreased by 33–43%.

RA-V decreased the protein levels of cyclin B1, cyclin D1, MMP2, VEGF-R1, VEGF-R2 and Tie 2 in endothelial cells

As mentioned in the previous section, RA-V induced cell cycle arrest at G2/M phase in endothelial cells. In order to determine whether RA-V was able to inhibit cyclin production, Western blotting experiments were performed in HUVEC and

HMEC-1. The results showed that RA-V (10–20 nM) significantly decreased the production of cyclin B1 and cyclin D1 after 24 h treatment in HUVEC and HMEC-1 (Figure 8A–D). On the other hand, RA-V (20 nM) significantly reduced active-MMP-2 production in both cell lines, while MMP-9 production was not significantly changed by RA-V treatment (Figure 8C, D).

Since binding of VEGF to its receptors, VEGF-R1 and VEGF-R2, is known to initiate angiogenesis, the effects of RA-V on the expression of these receptors were examined in Western blotting experiments. As shown in Figure 8A and E, RA-V (10–20 nM) decreased the expression of VEGFR1 and pVEGFR2 in HUVEC. The expression of VEGFR1 was significantly decreased in RA-V-treated HMEC-1, while that of pVEGFR2 was only slightly reduced (Figure 8B, F). The protein expression of tyrosine kinase receptor Tie2 in RA-V-treated endothelial cells was also assessed. As shown in Figure 8A, B, E and F, RA-V (20 nM) significantly decreased the protein level of Tie 2 in HUVEC and HMEC-1 cells.

RA-V reduces the phosphorylation of ERK1/2 in endothelial cells

To evaluate the effects of RA-V on intracellular signal transduction, the phosphorylation level of ERK1/2, JNK, and p38 MAPK were examined in both endothelial cell lines. The results showed that 10 and 20 nM RA-V inhibited the phosphorylation of ERK1/2 in a dose-dependent manner in HUVEC (Figure 9A, C) and HMEC-1 (Figure 9B, D).

On the other hand, RA-V significantly reduced the phosphorylation of JNK in HUVEC by about 30–40% (Figure 9C); however, no significant change of pJNK protein level observed in HMEC-1 (Figure 9B). The levels of total JNK were not affected by RA-V. Instead, treatment with 10 and 20 nM RA-V significantly reduced the phosphorylation of p38 MAPK and PI3K in HMEC-1 (Figure 9B, D, E). In addition, the p21 protein level was significantly increased in RA-V treated HMEC-1 (Figure 9E), while the increase of p21 in HUVEC was not statistically significant (Figure 9C).

Effects of RA-V on angiogenic gene expression in endothelial cells

The expression of several angiogenic genes (for Ang 1, Ang 2, Tie 2, VEGFR-2, MMP-2 and MMP-9) in RA-V-treated HUVEC and HMEC-1 cells was investigated by real-time PCR analysis. As shown in Figure 10A and B, both endothelial cell lines treated with RA-V (20 nM) for 24 h showed significant reductions of the mRNA levels of Tie 2 and VEGFR-2 ($P < 0.05$), which are the receptors for the angiogenic molecules. The reduction of VEGFR-2 mRNA levels in HUVEC was greater than that in HMEC-1 (64% vs. 32%). In addition, the treatment of RA-V also suppressed the mRNA expression levels of MMP-2 and MMP-9 in HUVEC by 52% and 45% respectively. There were greater reductions of MMP-2 and MMP-9 mRNA expression in HMEC-1, which were 80% and 55% respectively. Besides, RA-V treatment significantly reduced the expression of Ang 1 in both cell lines, while it reduced Ang 2 in HMEC-1 only. In contrast, an increase in Ang 2 mRNA expression was observed in HUVEC treated with RA-V; however, the changes were not statistically significant ($P > 0.05$).

RA-V reduces the phosphorylation of IκB-α in endothelial cells

To evaluate the effects of RA-V on NF-κB signal transduction, the TNF-α-induced phosphorylation level of IκB-α was examined in the whole cell extracts of endothelial cells. The results showed that 10 and 20 nM RA-V inhibited the phosphorylation of IκB in a dose-dependent manner in HUVEC (Figure 11A, C) and HMEC-1 (Figure 11B, D). The NF-κB in whole-cell extract was also decreased by RA-V (20 nM) treatment (Figure 11A–D).

RA-V inhibited angiogenesis in the Matrigel plug model

To further verify the inhibitory effect of RA-V on angiogenesis, the *in vivo* Matrigel plug assay was performed. The plugs containing VEGF and heparin exhibited a red colour indicating that new blood vessel formation (angiogenesis) occurred in the plugs (Figure S3). In the presence of RA-V, plugs were of light red or pale yellow colour, indicating that fewer blood vessels were formed. The extent of angiogenesis was quantified by measuring the haemoglobin content in the plugs. Figure 12 showed that the haemoglobin concentration in the plugs loaded with VEGF plus 100 nM RA-V was significantly lower than that in the plugs loaded with VEGF alone ($P < 0.05$). The result is consistent with the suppression of VEGF-induced angiogenesis by RA-V *in vitro*.

Discussion

RA-V has previously been demonstrated as a candidate anti-tumour agent (Itokawa *et al.*, 1983, 1984a, 1993); however, its inhibitory effect on angiogenesis in endothelial cells remains unknown. In the present study, the anti-angiogenic activities of RA-V isolated from *R. yunnanensis* were demonstrated for the first time in a number of cell culture assays using HUVEC and HMEC-1. Importantly, the mechanisms of action of RA-V in both endothelial cell lines *in vitro* have not been reported. Our results showed that the effective anti-angiogenic actions of RA-V were observed using low concentrations (10 or 20 nM), which did not cause cytotoxicity in endothelial cells after 24 h treatment. The results suggested that RA-V reduced the phosphorylation of ERK1/2 in both endothelial cell lines. In addition, the present results revealed the differential suppressive responses to RA-V by the two endothelial cell lines, which have distinct receptor levels and responses to endogenous ligands (Gerritsen, 1987; Aird, 2007).

As RA-V was initially investigated as an anti-tumour agent, its cytotoxicity in endothelial cells was also examined. Based on the results of the tested cancer cell lines, such concentrations (1–10 nM) of RA-V could significantly inhibit proliferation of HUVEC with cytotoxicity. Therefore, it is possible that RA-V can exert both anti-tumour and anti-angiogenesis effects on tumour treatment.

New vessel formation (angiogenesis) involves a multistep process, including cell proliferation, migration, tube assembly and remodelling. Suppression at any step may result in inhibition of angiogenesis (Cho *et al.*, 2009). Our results showed that the inhibitory effect of RA-V on proliferation was stronger in HUVEC than that in HMEC-1. The cell cycle

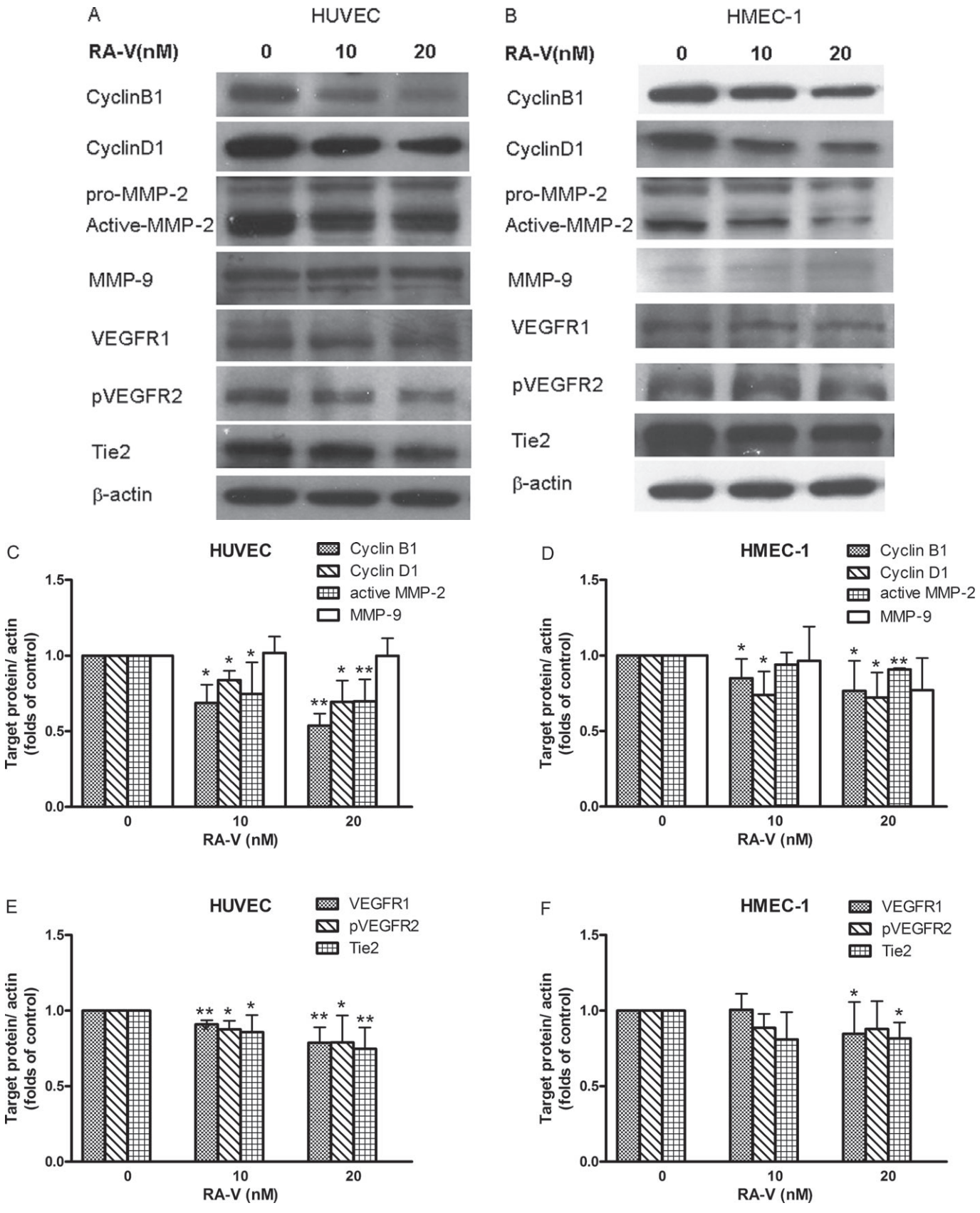
A
HUVEC
RA-V(nM) 0 10 20
CyclinB1
CyclinD1
pro-MMP-2
Active-MMP-2
MMP-9
VEGFR1
pVEGFR2
Tie2
β-actin
B
HMEC-1
RA-V(nM) 0 10 20
CyclinB1
CyclinD1
pro-MMP-2
Active-MMP-2
MMP-9
VEGFR1
pVEGFR2
Tie2
β-actin
C
HUVEC
Cyclin B1
Cyclin D1
active MMP-2
MMP-9
Target protein/ actin (folds of control)
RA-V (nM)
D
HMEC-1
Cyclin B1
Cyclin D1
active MMP-2
MMP-9
Target protein/ actin (folds of control)
RA-V (nM)
E
HUVEC
VEGFR1
pVEGFR2
Tie2
Target protein/ actin (folds of control)
RA-V (nM)
F
HMEC-1
VEGFR1
pVEGFR2
Tie2
Target protein/ actin (folds of control)
RA-V (nM)

Figure 8

Western blot analysis of the effects of RA-V on the expression of cyclins, MMPs, VEGFRs and Tie 2. HUVEC or HMEC-1 cells were synchronized in medium for 24 h and then treated with or without 10 or 20 nM RA-V for another 24 h or 48 h. Immunoblotting was performed three to four times using independently prepared cell lysates, and these are the representative blots of HUVEC (A) and HMEC-1 (B). The histograms (C–F) show the quantified results of protein levels, which were adjusted with corresponding β-actin protein level and expressed as fold of control (mean fold of control + SD of three to four independent experiments). Differences between the treated and untreated control groups were determined by Student's unpaired *t*-test. $^{*}P < 0.05$, $^{**}P < 0.01$ significantly different from the control group.

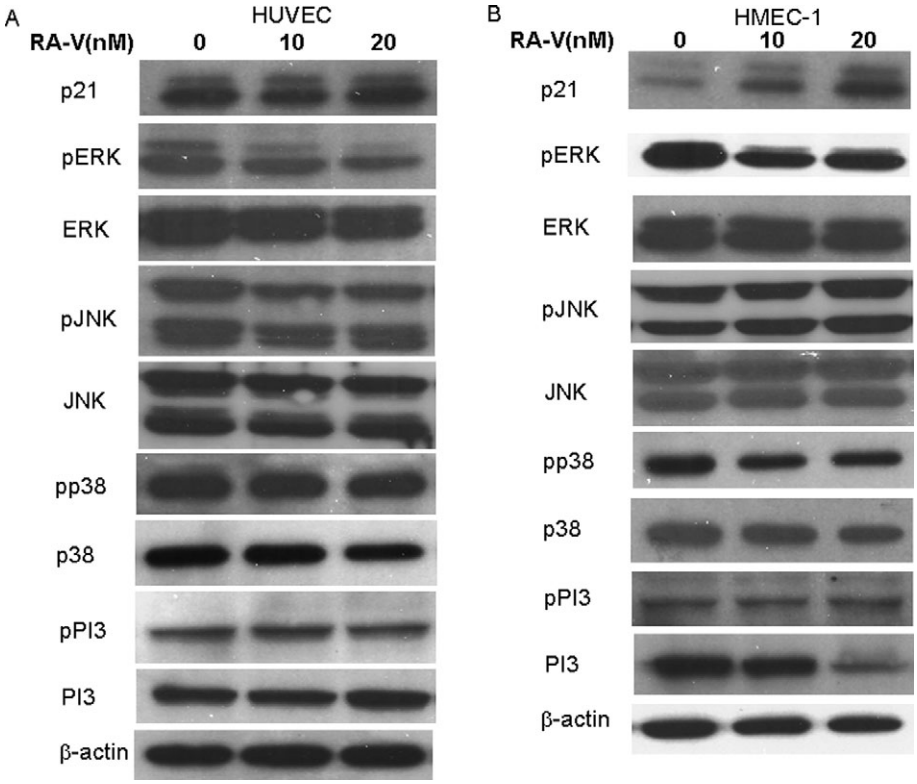

Figure 9

Western blot analyses of effect of RA-V on signalling kinases. HUVEC or HMEC-1 cells were synchronized in medium for 24 h and then treated with or without 10 or 20 nM RA-V for another 24 h or 48 h. Immunoblotting was performed three to four times using independently prepared cell lysates, and representative blots of HUVEC (A) and HMEC-1 (B) are shown. The histograms (C–E) show the quantified results of protein levels, which were adjusted with corresponding β-actin protein level and expressed as fold of control (mean fold of control + SD of three to four independent experiments). Differences between the treated and untreated control groups were determined by Student's unpaired *t*-test. $^{*}P < 0.05$, $^{**}P < 0.01$ significantly different from the control group.

distribution was analysed in RA-V-treated endothelial cells, which were also stimulated with or without growth factors, such as VEGF (10 ng mL^{-1}), bFGF (50 ng mL^{-1}) or serum (10% v/v). As shown in Figure 3, RA-V treatment induced G2/M phase cell cycle arrests in VEGF- and bFGF-stimulated HUVEC as well as serum- and bFGF-stimulated HMEC-1. Besides, both endothelial cell lines were arrested at G2/M phase in the absence of serum. In contrast, there was no significant change in cell cycle phase distribution after RA-V treatment in serum-stimulated (in basal medium) HUVEC and VEGF-stimulated HMEC-1 (data not shown). Basal proliferation of HUVEC is very low but can be effectively stimulated by VEGF or bFGF, while HMEC-1 proliferate spontaneously, but are not further stimulated by growth factors (Nanobashvili *et al.*, 2003). Our results are compatible with these earlier observations in that significant changes of the cell cycle were observed in VEGF- and bFGF-stimulated, but not in serum-stimulated, HUVEC. Similarly, the tube formation of VEGF- and bFGF-stimulated HUVEC was significantly reduced by RA-V (Figure 4A). As the production of VEGF-R1 was low in HMEC-1, the cells were more sensitive to bFGF than VEGF stimulation (Nanobashvili *et al.*, 2003). Hence, serum- and bFGF-stimulated HMEC-1 suffered cell cycle arrest after RA-V treatment (Figure 3F, G). RA-V treatment could also cause cell cycle arrest (Figure 3E, H) and inhibition of tube formation in both endothelial cell lines (Figures 4, S1), suggesting RA-V could inhibit angiogenesis in serum-free condition.

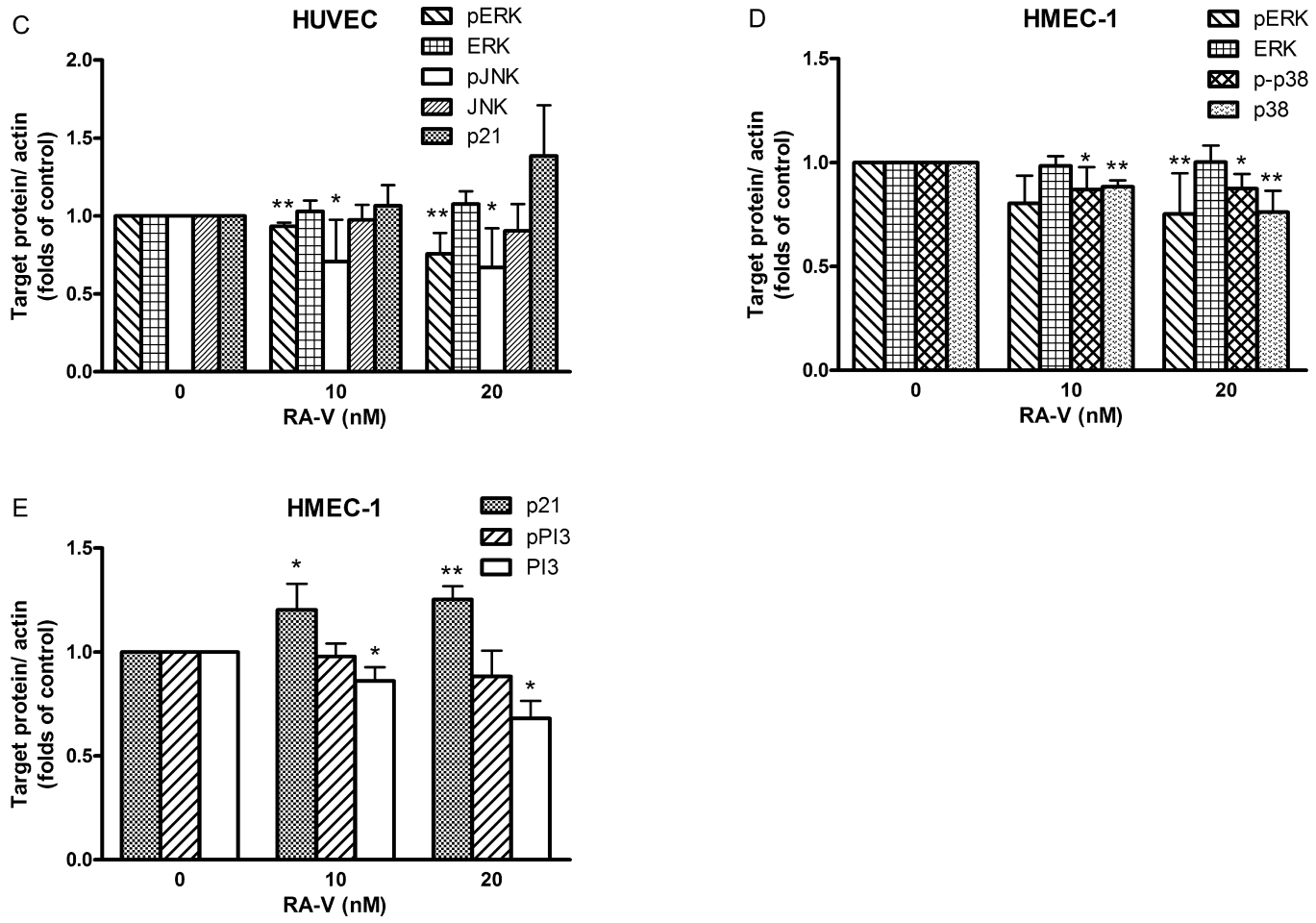

Figure 9

Continued.

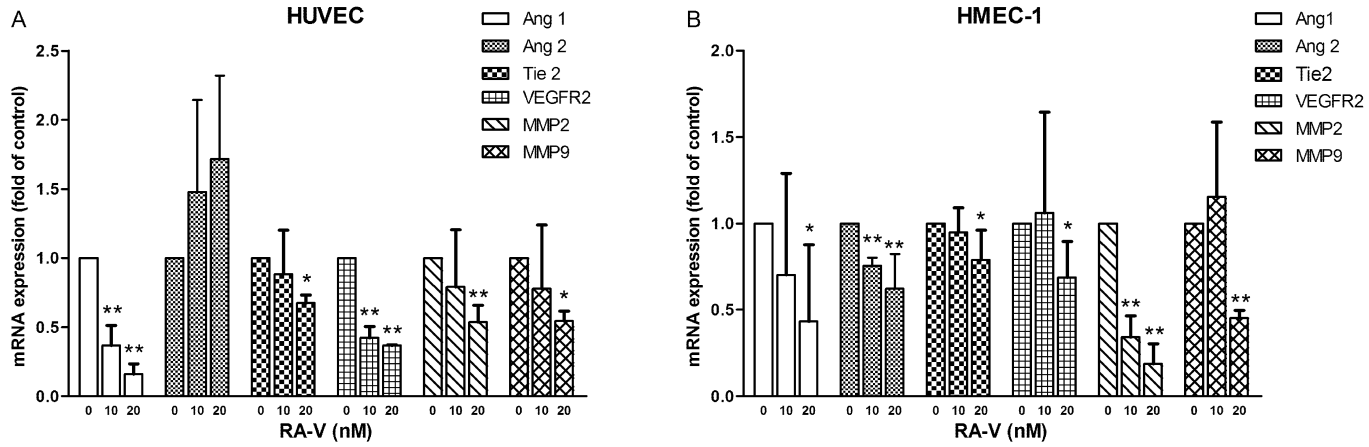

Figure 10

qRT-PCR analysis of angiogenic gene mRNA. HUVEC or HMEC-1 cells were synchronized in medium for 24 h and then treated with or without 10 or 20 nM RA-V for another 24 h. Data were normalized to GAPDH and untreated control. Results are expressed as fold of control (mean fold of control + SD from three to four independent experiments). Differences between the treated and untreated control groups were determined by Student's unpaired *t*-test. $*P < 0.05$, $**P < 0.01$ significantly different from the control group.

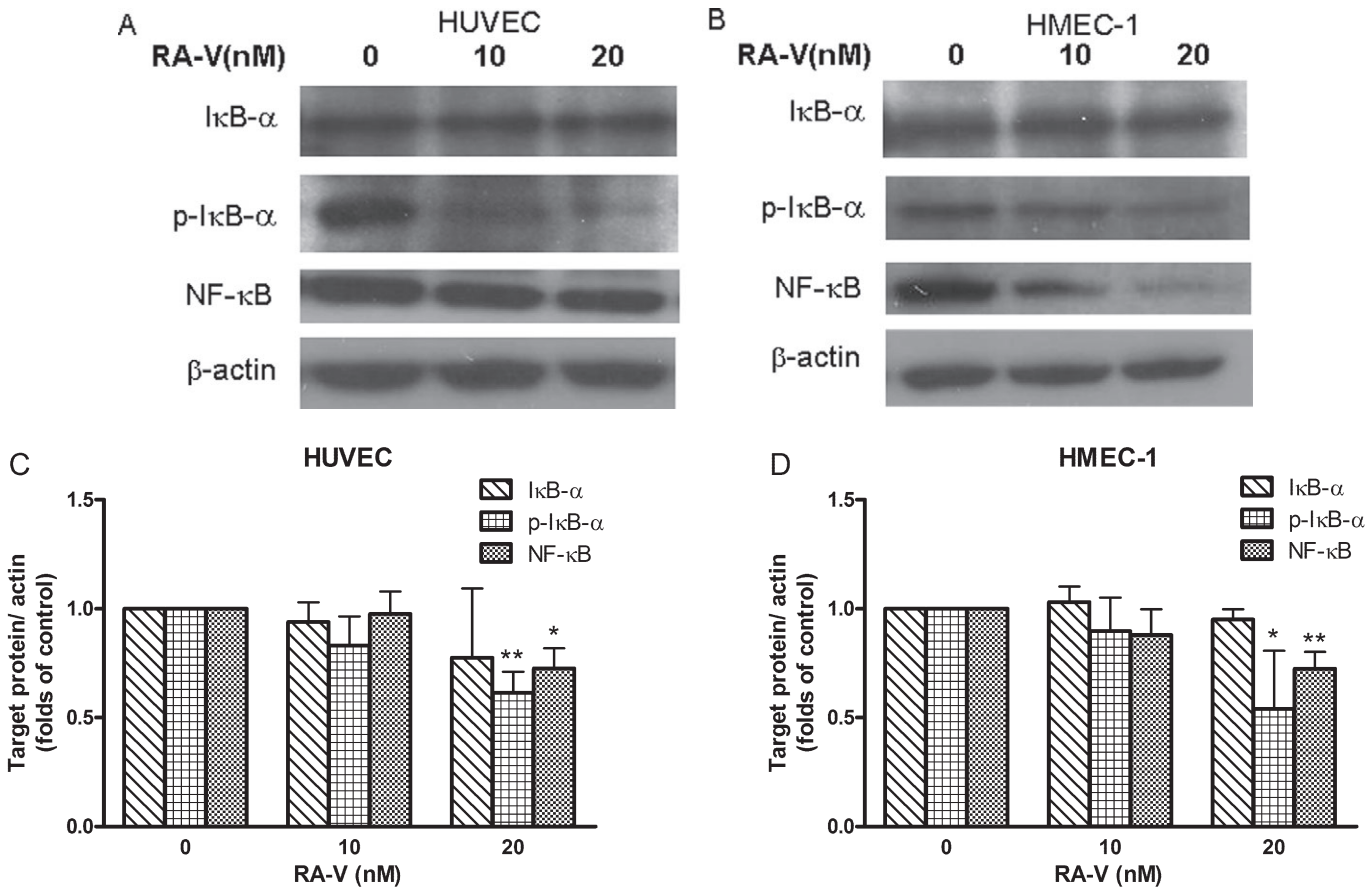

Figure 11

Western blot analyses of effect of RA-V on IκB phosphorylation. HUVEC or HMEC-1 cells were synchronized in medium for 24 h and then treated with or without 10 or 20 nM RA-V for 3 h and then treated with 10 ng mL^{-1} TNF-α for 30 min. Immunoblotting was performed three times using independently prepared whole cell lysates, and these are the representative blots of HUVEC (A) and HMEC-1 (B). The histograms (C and D) show the quantified results of protein levels, which were adjusted with corresponding β-actin protein level and expressed as fold of control (mean fold of control + SD of three independent experiments). Differences between the treated and untreated control groups were determined by Student's unpaired *t*-test. $*P < 0.05$, $**P < 0.01$ significantly different from the control group.

Assays of endothelial cell migration showed that RA-V inhibited the chemotactic response of endothelial cells. In another migration/wound-induced motility assay, RA-V significantly increased the open wound area, suggesting the motility of endothelial cells across wounds was inhibited. The inhibition of RA-V on HMEC-1 tube formation and migration was not due to cytotoxicity as there was no toxic effect observed after treating with RA-V for a relatively short period of time (5 h or 16 h; data not shown).

To further investigate mechanisms through which RA-V may exert their inhibitory effects on invasion and migration of endothelial cells, the effects of RA-V on the ability of HUVEC and HMEC-1 to adhere to ECM proteins were examined. RA-V decreased the ability of the cells to adhere to collagen type IV, fibronectin and vitronectin in the tested cell lines (Figure 7). Collagen IV plays an important role in cell adhesion and motility (Glynn *et al.*, 2008). Fibronectin has an important role in promoting endothelial cell survival and migration. It has also been shown to bind and enhance VEGF activity in mediating endothelial cell migration (Wijelath *et al.*, 2002). Vitronectin is a high molecular weight glycoprotein and known to promote cell adhesion and affect cell migration (Glynn *et al.*, 2008). Hence, treatment with RA-V resulted in decreased adhesion of endothelial cells to these matrix proteins and such effects were seldom demonstrated by other anti-angiogenic candidates.

Degradation of the underlying basement membrane by endothelial cells of the existing blood vessels is a crucial step for initiating the formation of new capillaries (Carmeliet, 2000). Such process requires the cooperative activity of the MMP system. MMP-2 and MMP-9 are specific for the degradation of type IV collagen. Type I and V collagen, laminin and fibronectin are also the substrates of MMP-2 (Liekens *et al.*, 2001). In the present study, the changes in protein and mRNA expression levels of pro- and active MMP-2 and MMP-9 have been determined. The protein levels and mRNA expression of active MMP-2 in both endothelial cell lines were significantly decreased after 24 h of RA-V treatment (Figures 8C, D, 10A, B), whereas the RA-V-induced changes of MMP-9 protein level were observed only after 72 h treatment (data not shown). Nonetheless, the mRNA expression of MMP-9 was decreased in RA-V-treated endothelial cells

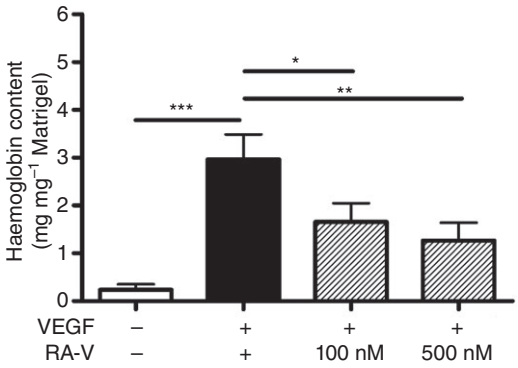

Figure 12

Effect of RA-V on VEGF-induced *in vivo* angiogenesis in Matrigel plugs. Haemoglobin content of Matrigel plugs from groups of mice, treated as indicated. Results are expressed as the mean + SEM (n = 13) of three independent experiments. Differences between the VEGF alone group and untreated control group as well as VEGF plus RA-V groups were determined by Student's unpaired t-test. *P < 0.05; **P < 0.01; ***P < 0.005.

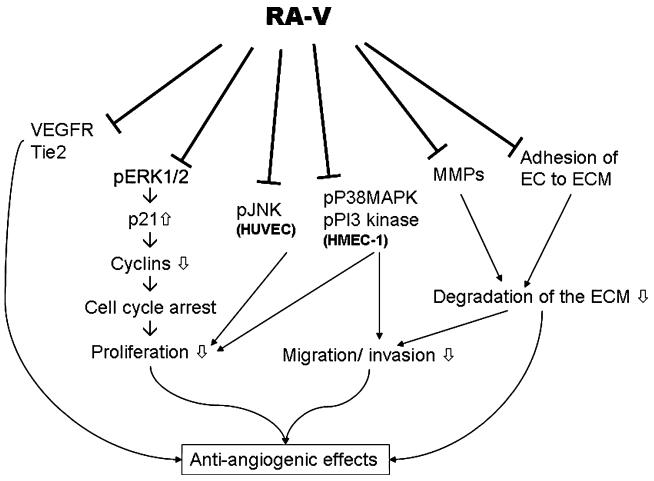

Figure 13

Scheme outlining actions of RA-V on different cellular components involved in anti-angiogenesis in endothelial cells.

(Figure 10A, B). Inhibition of active MMP-2 and MMP-9 expression and decreased adhesion of endothelial cells to ECM by RA-V may cooperate to reduce degradation of ECM and thereby inhibit angiogenesis.

Apart from the effects of RA-V on the MMP system, we hypothesized that RA-V suppresses the endothelial cell proliferation by activating p21 and inactivating ERK1/2. Our results showed that, the protein level of p21 increased to different extents in RA-V-treated HUVEC and HMEC-1. Meanwhile, RA-V suppressed ERK1/2 phosphorylation in both cell lines. Interestingly, significant decrease in phosphorylation of p38 MAPK and PI3K were observed in RA-V-treated HMEC-1 only. Such changes of signalling molecules may be responsible for the inhibition of proliferation and migration as well as cell cycle arrest in endothelial cells. On the other hand, decreased JNK/SPAK phosphorylation was observed in RA-V-treated HUVEC only. The JNK may act as the final mediator of ERK1/2 to control cell proliferation (Hsu *et al.*, 2009) and matrix regulation (Medhora *et al.*, 2008). On the other hand, the protein and mRNA expression of receptors for angiogenic molecules (VEGFR1, VEGFR2 and Tie 2) were decreased in RA-V-treated endothelial cells. In addition, the mRNA expression of Ang 1, which is angiogenic (Carmeliet, 2000), was down-regulated by RA-V treatment in both endothelial cell lines. Such changes may play a role in the anti-angiogenic effect of RA-V. In contrast, changes in Ang 2 mRNA expression was different in the two types of endothelial cells. Treatment of RA-V induced up-regulation of Ang 2 in HUVEC but down-regulation in HMEC-1. These differential responses may due to the different production of endogenous VEGF in the two cell types. HMEC-1 but not HUVEC produces VEGF (Nanobashvili *et al.*, 2003). Ang 2 suppresses endothelial survival when there is no angiogenic stimulus (Carmeliet, 2000)but it promotes angiogenesis in the presence of angiogenic molecules (Adams and Alitalo, 2007). Therefore, when Ang 2 was up-regulated by RA-V in HUVEC, the survival of the cells was suppressed. On the other hand, in HMEC-1 (with endogenous VEGF), down-regulation of Ang 2 by RA-V resulted in anti-angiogenesis. The present study has provided novel and mechanistic insights into how RA-V targets many components of angiogenic signalling pathways. A scheme of possible mechanisms that underlie the actions of RA-V on endothelial cells is shown in Figure 13.

Earlier, RA-V inhibited NF-κB activation in human embryonic kidney HEK-293-NF-κB luciferase stable cells (Fan *et al.*, 2010). The effect of RA-V on NF-κB activation in endothelial cells was examined in the present study. The phosphorylation and degradation of IκB is one of the critical steps in NF-κB activation (Park *et al.*, 2007). Application of TNF-α can induce IκB phosphorylation and degradation in endothelial cells (Bieler *et al.*, 2007). Thus, the levels of IκB-α and phospho-IκB-α after TNF-α treatment were measured in RA-V-pretreated endothelial cells whole-cell extracts. Our results showed that RA-V (20 nM) treatment decreased the protein level of p-IκB, suggesting that RA-V may affect NF-κB activation, in both endothelial cell lines (Figure 11). Besides, the effect of RA-V on reactive oxygen species (ROS) production in endothelial cells was also evaluated as ROS play roles in the apoptosis and NF-κB activation in endothelial cells (Du *et al.*, 1999). However, there was no significant change in ROS production in the endothelial cells after RA-V-treatments (10 or 20 nM for 12, 24 or 48 h; data not shown). The results suggested that the inhibition of RA-V on the NF-κB pathway may not act through the inhibition of ROS production.

Furthermore, the *in vivo* anti-angiogenic effects of RA-V was studied using a mouse Matrigel plug model. RA-V decreased the haemoglobin content in Matrigel plugs loaded with VEGF in comparison with VEGF alone. These *in vivo* results substantiate the inhibitory effects of RA-V, which is able to prevent vascular endothelial cells from responding to VEGF.

In conclusion, the anti-angiogenic effects of RA-V on HUVEC and HMEC-1 cells may be exerted through inhibition of ERK1/2 phosphorylation and MMP activation, leading to decreased cell proliferation and migration/invasion, respec-

tively. RA-V may also exert anti-angiogenic activity by down-regulating the expression of VEGFR. In addition, the results of reducing PI3K signalling activities in HMEC-1 and JNK/SPAK phosphorylation in HUVEC have disclosed different responses to RA-V in the two endothelial cell lines. These findings may provide support for the potential use of RA-V as an anti-angiogenic therapy.

Acknowledgements

This research was supported in part of Ming Lai Foundation and the National Natural Science Foundation of China (30725048, 91013002, U1032602). The authors would like to thank Dr Erik Ko for the technical support on qRT-PCR analysis, and Dr Ben Chan and Dr Elaine Wat for the technical support on Western blotting analysis.

Conflict of interest

None.

References

Adams RH, Alitalo K (2007). Molecular regulation of angiogenesis and lymphangiogenesis. Nat Rev Mol Cell Biol 8: 464–478.

Aird WC (2007). Phenotypic heterogeneity of the endothelium: I. structure, function, and mechanisms. Circ Res 100: 158–173.

Alexander SPH, Mathie A, Peters JA (2009). Guide to Receptors and Channels (GRAC), 4th edition. Br J Pharmacol 158 (Suppl. 1): S1–S254.

Avramis IA, Kwock R, Avramis VI (2001). Taxotere and vincristine inhibit the secretion of the angiogenesis inducing vascular endothelial growth factor (VEGF) by wild-type and drug-resistant human leukemia T-cell lines. Anticancer Res 21: 2281–2286.

Bates RB, Cole JR, Hoffmann JJ, Kriek GR, Linz GS, Torrance SJ (1983). Solution forms of bouvardin and relatives from NMR studies. 6-*O*-Methylbouvardin. J Am Chem Soc 105: 1343–1347.

Bieler G, Hasmim M, Monnier Y, Imaizumi N, Ameyar M, Bamat J *et al*. (2007). Distinctive role of integrin-mediated adhesion in TNF-induced PKB/Akt and NF-kappaB activation and endothelial cell survival. Oncogene 26: 5722–5732.

Carmeliet P (2000). Mechanisms of angiogenesis and arteriogenesis. Nat Med 6: 389–395.

Carmeliet P, Jain RK (2000). Angiogenesis in cancer and other diseases. Nature 407: 249–257.

Chia JS, Du JL, Hsu WB, Sun A, Chiang CP, Wang WB (2010). Inhibition of metastasis, angiogenesis, and tumor growth by Chinese herbal cocktail Tien-Hsien Liquid. BMC Cancer 10: 175.

Cho SG, Yi Z, Pang X, Yi T, Wang Y, Luo J *et al*. (2009). Kisspeptin-10, a KISS1-derived decapeptide, inhibits tumor angiogenesis by suppressing Sp1-mediated VEGF expression and FAK/Rho GTPase activation. Cancer Res 69: 7062–7070.

Clements MK, Jones CB, Cumming M, Daoud SS (1999). Antiangiogenic potential of camptothecin and topotecan. Cancer Chemother Pharmacol 44: 411–416.

Conway EM, Carmeliet P (2004). The diversity of endothelial cells: a challenge for therapeutic angiogenesis. Genome Biol 5: 207.

Crum R, Szabo S, Folkman J (1985). A new class of steroids inhibits angiogenesis in the presence of heparin or a heparin fragment. Science 230: 1375–1378.

Du X, Stocklauser-Färber K, Rösen P (1999). Generation of reactive oxygen intermediates, activation of NF-kappaB, and induction of apoptosis in human endothelial cells by glucose: role of nitric oxide synthase? Free Radic Biol Med 27: 752–763.

Fan JT, Su J, Peng YM, Li Y, Li J, Zhou YB *et al*. (2010). Rubiyunnanins C-H, cytotoxic cyclic hexapeptides from *Rubia yunnanensis* inhibiting nitric oxide production and NF-κB activation. Bioorg Med Chem 18: 8226–8234.

Fan TP, Yeh JC, Leung KW, Yue PY, Wong RN (2006). Angiogenesis: from plants to blood vessels. Trends Pharmacol Sci 27: 297–309.

Folkman J (1971). Tumor angiogenesis: therapeutic implications. N Engl J Med 285: 1182–1186.

Folkman J (2007). Angiogenesis: an organizing principle for drug discovery? Nat Rev Drug Discov 6: 273–286.

Gerritsen ME (1987). Functional heterogeneity of vascular endothelial cells. Biochem Pharmacol 36: 2701–2711.

Glynn SA, O'Sullivan D, Eustace AJ, Clynes M, O'Donovan N (2008). The 3-hydroxy-3-methylglutaryl-coenzyme A reductase inhibitors, simvastatin, lovastatin and mevastatin inhibit proliferation and invasion of melanoma cells. BMC Cancer 8: 9.

He MF, Huang YH, Wu LW, Ge W, Shaw PC, But PP (2010). Triptolide functions as a potent angiogenesis inhibitor. Int J Cancer 126: 266–278.

Hsu SC, Ou CC, Chuang TC, Li JW, Lee YJ, Wang V *et al*. (2009). *Ganoderma tsugae* extract inhibits expression of epidermal growth factor receptor and angiogenesis in human epidermoid carcinoma cells: *In vitro* and *in vivo*. Cancer Lett 281: 108–116.

Itokawa H, Takeya K, Mihara K, Mori N, Hamanaka T, Sonobe T *et al*. (1983). Studies on the antitumor cyclic hexapeptides obtained from *Rubiae radix*. Chem Pharm Bull (Tokyo) 31: 1424–1427.

Itokawa H, Takeya K, Mori N, Hamanaka T, Sonobe T, Mihara K (1984a). Isolation and antitumor activity of cyclic hexapeptides isolated from *Rubiae radix*. Chem Pharm Bull (Tokyo) 32: 284–290.

Itokawa H, Takeya K, Mori N, Sonobe T, Serisawa N, Hamanaka T *et al*. (1984b). Studies on antitumor cyclic hexapeptides RA obtained from *Rubiae radix*, Rubiaceae. III. On derivatives of RA-V and their *in vivo* activities. Chem Pharm Bull (Tokyo) 32: 3216–3226.

Itokawa H, Kondo K, Hitotsuyanagi Y, Nakamura A, Morita H, Takeya K (1993). Preparation and cytotoxicity of cyclic hexapeptides, RA derivatives. Chem Pharm Bull (Tokyo) 41: 1266–1269.

Jolad SD, Hoffmann JJ, Torrance SJ, Wiedhopf RM, Cole JR, Arora SK *et al*. (1977). Bouvardin and deoxybouvardin, antitumor cyclic hexapeptides from *Bouvardia ternifolia* (Rubiaceae). J Am Chem Soc 99: 8040–8044.

Kimura Y, Sumiyoshi M, Baba K (2008). Antitumor activities of synthetic and natural stilbenes through antiangiogenic action. Cancer Sci 99: 2083–2096.

Koizumi T, Abe M, Yamakuni T, Ohizumi Y, Hitotsuyanagi Y, Takeya K *et al*. (2006). Metronomic scheduling of a cyclic hexapeptide Ra-VII for anti-angiogenesis, tumor vessel maturation and anti-tumor activity. Cancer Sci 97: 665–674.

Lee JE, Hitotsuyanagi Y, Kim IH, Hasuda T, Takeya K (2008). A novel bicyclic hexapeptide, RA-XVIII, from *Rubia cordifolia*: structure, semi-synthesis, and cytotoxicity. Bioorg Med Chem Lett 18: 808–811.

Lee JH, Choi S, Lee Y, Lee HJ, Kim KH, Ahn KS *et al*. (2010a). Herbal compound farnesiferol C exerts antiangiogenic and antitumor activity and targets multiple aspects of VEGFR1 (Flt1) or VEGFR2 (Flk1) signaling cascades. Mol Cancer Ther 9: 389–399.

Lee YS, Kim YH, Shin EK, Kim DH, Lim SS, Lee JY *et al*. (2010b). Anti-angiogenic activity of methanol extract of *Phellinus linteus* and its fractions. J Ethnopharmacol 131: 56–62.

Liekens S, De Clercq E, Neyts J (2001). Angiogenesis: regulators and clinical applications. Biochem Pharmacol 61: 253–270.

Medhora M, Dhanasekaran A, Pratt PF, Jr, Cook CR, Dunn LK, Gruenloh SK *et al*. (2008). Role of JNK in network formation of human lung microvascular endothelial cells. Am J Physiol Lung Cell Mol Physiol 294: L676–L685.

Nanobashvili J, Jozkowicz A, Neumayer C, Fiigl A, Sporn E, Polterauer P *et al*. (2003). Comparison of angiogenic potential of human microvascular endothelial cells and human umbilical vein endothelial cells. Eur Surg 35: 214–218.

Park JM, Kim A, Oh JH, Chung AS (2007). Methylseleninic acid inhibits PMA-stimulated pro-MMP-2 activation mediated by MT1-MMP expression and further tumor invasion through suppression of NF-kappaB activation. Carcinogenesis 28: 837–847.

Tan NH, Zhou J (2006). Plant cyclopeptides. Chem Rev 106: 840–895.

Tao J, Morikawa T, Ando S, Matsuda H, Yoshikawa M (2003). Bioactive constituents from Chinese natural medicines. XI. inhibitors on NO production and degranulation in RBL-2H3 from *Rubia yunnanensis*: structures of rubianosides II, III, and IV, rubianol-g, and rubianthraquinone. Chem Pharm Bull (Tokyo) 51: 654–662.

Taylor S, Folkman J (1982). Protamine is an inhibitor of angiogenesis. Nature 297: 307–312.

Vigl B, Zgraggen C, Rehman N, Banziger-Tobler NE, Detmar M, Halin C (2009). Coxsackie- and adenovirus receptor (CAR) is expressed in lymphatic vessels in human skin and affects lymphatic endothelial cell function *in vitro*. Exp Cell Res 315: 336–347.

Vincent L, Kermani P, Young LM, Cheng J, Zhang F, Shido K *et al*. (2005). Combretastatin A4 phosphate induces rapid regression of tumor neovessels and growth through interference with vascular endothelial-cadherin signaling. J Clin Invest 115: 2992–3006.

Wijelath ES, Murray J, Rahman S, Patel Y, Ishida A, Strand K *et al*. (2002). Novel vascular endothelial growth factor binding domains of fibronectin enhance vascular endothelial growth factor biological activity. Circ Res 91: 25–31.

Xiao D, Singh SV (2007). Phenethyl isothiocyanate inhibits angiogenesis *in vitro* and *ex vivo*. Cancer Res 67: 2239–2246.

Yue GGL, Chan BC, Hon PM, Lee MY, Fung KP, Leung PC *et al*. (2010). Evaluation of in vitro anti-proliferative and immunomodulatory activities of compounds isolated from *Curcuma longa*. Food Chem Toxicol 48: 2011–2020.

Zhang C, Yang F, Zhang XW, Wang SC, Li MH, Lin LP *et al*. (2006). *Grateloupia longifolia* polysaccharide inhibits angiogenesis by downregulating tissue factor expression in HMEC-1 endothelial cells. Br J Pharmacol 148: 741–751.

Supporting information

Additional Supporting Information may be found in the online version of this article:

Figure S1 Effects of RA-V on capillary-like tube formation by HUVEC and HMEC-1. Representative photomicrographs showing the VEGF-induced tube structures of HUVEC or HMEC-1 following 16 h or 5 h treatments, respectively, with DMSO (0 nM/control) or indicated concentrations of RA-V.
Figure S2 Effects of RA-V on wound-induced motility of HUVEC and HMEC-1. Representative photomicrographs showing the cells migrated across the scratch wound in the presence or absence of RA-V after 16 h incubation.
Figure S3 Effect of RA-V on VEGF-induced *in vivo* angiogenesis in Matrigel plugs. The representative pictures of Matrigel plugs from indicated groups at day 7 after inoculation into mice.
Table S1 Gene-specific PCR primers
Table S2 ^{1}H NMR (500 MHz) and ^{13}C NMR (100 MHz) data for RA-V in $CDCl_3$ (δ in ppm, J in Hz)

Please note: Wiley-Blackwell are not responsible for the content or functionality of any supporting materials supplied by the authors. Any queries (other than missing material) should be directed to the corresponding author for the article.